EVAPORATION FROM DROPS

Part I

W. E. RANZ* and W. R. MARSHALL, JR.

University of Wisconsin, Madison, Wisconsin

An investigation was made of the factors influencing the rate of evaporation of pure liquid drops, and the rate of evaporation of water drops containing dissolved and suspended solids. The study was restricted to a Reynolds number range of 0 to 200, the range usually encountered in spray-drying operations. Independent correlations of heat- and mass-transfer rates were obtained from drop temperatures measured with 0.5 mil thermocouples. Drop diameters ranged from 0.06 to 0.11 cm., and air temperatures up to 220° C.

Results of studies on pure liquid drops confirmed the analogy between heat and mass transfer at low Reynolds numbers, and verified the simple expression for the Nusselt number at zero Reynolds number. A general correlation of existing data on spherical particles showed the results of this study could be extrapolated with remarkable accuracy five times beyond the experimental range of Reynolds numbers.

Studies on water drops containing dissolved and suspended solids furnished a preliminary insight into the mechanism of the formation of particles dried from drops. The results showed that when the solid was in solution the drop evaporated initially as though it were saturated throughout, even though its average concentration was less than saturation. This was shown to be true for solutions of ammonium nitrate and sodium chloride, and a convenient method for estimating the drop temperature and evaporation rate for this case was proposed. For drops containing insoluble materials, the initial evaporation rate was found to correspond to that for pure water. When the drop formed a solid structure and its diameter became constant, the falling-rate period ensued during which the drop temperature rose continually. This temperature rise was due to both heat of crystallization and sensible heat transfer, in the case of solutions, and primarily to sensible heat transfer in the case of suspensions.

METHODS of predicting the evaporation rates of a single drop and the phenomena associated with the evaporation process are of importance in the analysis of chemical engineering operations involving dispersions in

* Present address: University of Illinois, Urbana, Ill.

gases. Fundamental data on the factors affecting the rate of heat and mass transfer for a spray droplet are important to the operations of spray drying, spray cooling, humidification, spray absorption, spray extraction, combustion, crystallization, dissolution, transfer in fluidized beds, and any other operation

where transfer occurs between a continuous phase and a discontinuous phase which appears as spherical particles.

The purpose of this paper is to report a fundamental study of evaporation from drops. This study was divided into the following parts:

1. Rate of heat transfer to the drop surface.
2. Rate of evaporation and mass transfer from the drop surface.
3. Temperature and concentration at the drop surface during evaporation.
4. Effect on evaporation rate of original drop temperature, heats of solution and crystallization, and the way in which solid surfaces form.

Application of the results has been made with specific reference to spray drying. In spray drying, as in most drying problems, the first period of drying, usually termed the constant-rate period, is susceptible to a simple analysis. However, as soon as a spray droplet concentrates to the point where it no longer presents a free liquid surface to the gas stream, it becomes a particle with drying characteristics determined by the nature of the solid structure. The particle then enters a period in which the rate of drying decreases with decreasing moisture content. For application to the operation of spray drying, this study was primarily concerned with the constant-rate period.

Review of Previous Work

Only a small amount of experimental work has been done on the fundamentals of heat and mass transfer in the evaporation of single drops. Experimental difficulties are evident when it is realized that drop diameters should be in the range of 200 to

800μ, and the Reynolds number range should be from 0 to 100 to approach conditions of commercial interest.

Kramers (17) recorded heat-transfer data for spheres in the low Reynolds number range. However, the diameters of the spheres he used were of the order of 1 cm., and free convection obscured the true effect of the velocity of the fluid stream. Meyer (23) presented an analysis of data on free convection from spheres in quiescent fluids of various kinds.

Evaporation of solid and liquid drops in still air has been treated from the standpoint of simple mass transfer. Experimental data of Morse (24) on the sublimation of iodine beads led to a calculation by Langmuir (18) of the diffusivity of iodine vapor in air. Fuchs (10) presented a theoretical treatment of mass transfer for evaporation of drops in still air.

Evaporation of droplets at finite air velocities was treated theoretically and experimentally by Froessling (9), but the results were based largely on the evaporation of materials of low volatility so that the problem was essentially one of mass transfer only. Froessling's data along with other literature data were reviewed by Williams (29) who was primarily interested in the evaporation of mustard gas, a substance of low volatility.

As far as the evaporation of drops containing dissolved and suspended solids is concerned, the available data (32) are meager and inconclusive, and offer no basis for the prediction and explanation of phenomena associated with the constant-rate period. For the falling-rate period only the studies of Van Krevelin (27) on the drying of single particles seem applicable.

Theoretical Considerations

The evaporation of a liquid drop is essentially an operation in which heat for evaporation is transferred by conduction and convection from hot gases to the drop surface from which vapor is transferred by diffusion and convection back into the gas stream. The rate of transfer per unit area of interface is a function of the temperature, humidity, and transport properties of the gas, and the diameter, temperature, and relative velocity of the drop.

Boundary layer theory predicts that the rate of transfer is a maximum on the front side of the drop facing the oncoming air stream, decreases to a minimum value near the separation point, and increases to another, but lower, maximum rate on the trailing face which experiences velocities in the reverse direction. Such a distribution of mass-transfer rates was shown by Froessling (9) for the sublimation of a naphthalene bead.

Figure 1 shows a temperature difference exploration around an evaporating water drop. It is evident that the rate of heat transfer will be largest on the side facing the air stream where the temperature gradient is steepest and the isotherms are close together. This temperature exploration reveals the significant fact that the thickness of the boundary layer is, in general, of the same

order of magnitude as the diameter of the evaporating water drop. Thus, any theoretical development or empirical correlation should account for the variable cross-sectional area of transfer through the boundary layer.

Heat- and Mass-Transfer Equations for an Evaporating Drop. From Froessling's boundary layer equations for a blunt-nosed body of revolution (9) and from equations for heat and mass transfer, a set of four dimensionless partial differential equations can be developed for the evaporation of a liquid drop in an air stream. These may be written in dimensionless quantities as follows:

$$\left(\frac{1}{N_{Pr}N_{Re}}\right)\left\{\frac{1}{R^2}\frac{\partial}{\partial R}\left(R^2\frac{\partial T}{\partial R}\right) + \frac{1}{R^2 \sin\theta}\frac{\partial}{\partial R}\left(\sin\theta\frac{\partial T}{\partial\theta}\right)\right\} = \frac{V_r\partial T}{\partial R} + \frac{V_\theta\partial T}{R\partial\theta}$$

(Heat balance)   (1)

$$\left(\frac{\pi}{N_{Sc}N_{Re}p_f}\right)\left\{\frac{1}{R^2}\frac{\partial}{\partial R}\left(R^2\frac{\partial P_A}{\partial R}\right) + \frac{1}{R^2 \sin\theta}\frac{\partial}{\partial\theta}\left(\sin\theta\frac{\partial P_A}{\partial\theta}\right)\right\} = \frac{V_r\partial P_A}{\partial R} + \frac{V_\theta\partial P_A}{R\partial\theta}$$

(Mass balance on component A)   (2)

$$\frac{V_\theta\partial V_\theta}{R\partial\theta} + \frac{V_r\partial V_\theta}{\partial R} = -\frac{1}{R}\frac{\partial P}{\partial\theta} + \frac{1\partial^2 V_\theta}{N_{Re}\partial R^2}$$

(3)

(Force balance—modified Navier-Stokes equation)

$$\frac{1\partial}{R\partial\theta}(R \sin\theta V_\theta) + \frac{\partial}{\partial R}(R \sin\theta V_r) = 0$$

(4)

(Equation of continuity)

with boundary conditions:

(1) $T = P_A = 0$, $V_\theta = V_r = 0$, at $R = \frac{1}{2}$

(2) $T = P_A = 1.0$, at $R = \infty$; $V_\theta = v'_\theta/v_o$; $V_r = v'_r/v_o$, at $R > \delta/D_p$

where δ is the thickness of the boundary layer. Mathematically the boundary layer is defined as the region of velocities whose magnitudes are less than those for potential flow because of the retarding effect of friction at the interface.

A general solution of this formidable set of equations is not possible, and such a solution is not justified in view of the numerous assumptions which must be made regarding average physical properties across the transfer path, and in view of the existence of drop rotation, drop vibration, and unsteady-state phenomena. However, the heat-and mass-transfer numbers can be shown to take the theoretical and functional form

$$N_{Nu} = -\frac{1}{2}\int_0^\pi \left(\frac{\partial T}{\partial R}\right)_{R=\frac{1}{2}} \sin\theta d\theta = N_{Nu}(N_{Re}, (N_{Re}N_{Pr}))$$
$$= N_{Nu}'(N_{Re}, (N_{Re}N_{Pr}))$$

(5)

$$N_{Nu'} = -\frac{1}{2}\int_0^\pi \left(\frac{\partial P_A}{\partial R}\right)_{R=\frac{1}{2}} \sin\theta d\theta = N_{Nu}'\left(N_{Re}, \left(N_{Re}N_{Sc}\frac{p_f}{\pi}\right)\right)$$
$$= N_{Nu}\left(N_{Re}, \left(N_{Re}N_{Sc}\frac{p_f}{\pi}\right)\right)$$

(6)

The analogy shown by Equations (5) and (6) arises from the fact that Equations (1) and (2) are mathematically equivalent and subject to the same boundary conditions. Thus, N_{Nu} and N_{Nu}' should have exactly the same functional form where N_{Pr} for heat transfer is equivalent to $N_{Sc}p_f/\pi$ for mass transfer. This is an important conclusion, applicable to all heat- and mass-transfer problems where the rate of transfer is controlled by the boundary layer.

Since p_f/π is nearly unity in most applications, it is omitted as a factor on N_{Sc} in the material which follows and is implied only as a correction in broad extrapolations of recommended results.

Limiting Condition at Zero Reynolds Number. Since the physical situation in finely dispersed systems is such that the relative velocity and N_{Re} become vanishingly small, the limiting case for a drop evaporating in still air is of practical importance. For $v_\theta = v_r = 0$, Equations (1), (2), (5), and (6) give the relationship

$$N_{Nu} = N_{Nu}' = 2.0 \qquad (7)$$

From Equation (7) it can be shown that the rate of change of surface area

of a pure liquid drop is constant during evaporation and that the total lifetime of such a drop is proportional to the square of the original drop diameter, facts reported empirically and theoretically by many investigators (9, 10, 18, 29).

Forced Convection. For finite velocities several solutions based on simplifying assumptions have been proposed. Johnstone and Kleinschmidt (14) in an absorption study postulated a hypothetical tube of gas, described by the trace of the periphery of a liquid particle in motion through a gas, whose thickness is equal to the distance heat and/or mass can be transferred in the time it takes the particle to move through one diameter. Johnstone, Pigford and Chapin (15) developed a solution of the Boussinesq type for heat transfer. These simplified solutions failed to give a finite value of 2.0 for $N_{Re} = 0$. To obtain the proper limiting value of $N_{Nu} = 2.0$ at $N_{Re} = 0$, Johnstone, Pigford and Chapin (15) developed a solution to Equations (1) and (5) on the assumption that $V_\theta = 1.0$ and $V_r = 0$ at all $R > \frac{1}{2}$.

Experimental data on mass-transfer rates for spheres may be correlated by an empirical equation of the form used by Froessling (9):

$$N_{Nu}' = 2.0 + K_1(N_{Sc})^m(N_{Re})^n$$

(8)

where K_1 is a constant, $m = \frac{1}{3}$ and $n = \frac{1}{2}$. By analogy heat-transfer data should be correlated by a corresponding equation:

$$N_{Nu} = 2.0 + K_2(N_{Pr})^p(N_{Re})^q$$

(9)

where

$$K_1 = K_2, p = m = \frac{1}{3},$$

and

$$q = n = \frac{1}{2}.$$

Equations (8) and (9) are both consistent with the theoretical requirement that $N_{Nu} = N_{Nu}' = 2$ at $N_{Re} = 0$. At high values of N_{Re}, the constant term becomes less significant, so that Equations (8) and (9) may be converted to the familiar j-factor equations of Chilton and Colburn (4).

Free Convection. At zero relative velocity, if heat transfer is by simple conduction and mass transfer is by simple diffusion, $N_{Nu} = N_{Nu}' = 2.0$. In the practical case, however, a density difference exists across the transfer path, and a fluid velocity caused by free convection contributes to the transfer rate. To account for this effect, it is proposed
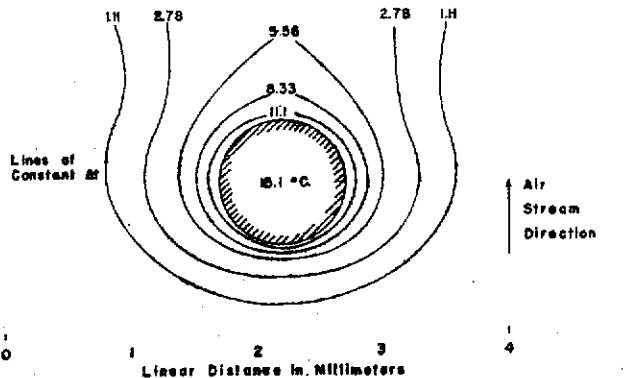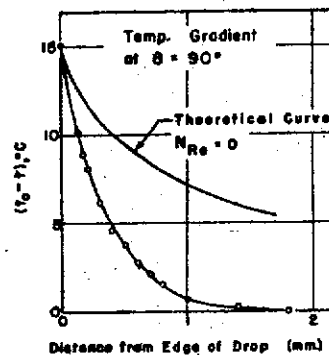

Fig. 1. Temperature exploration around an evaporating water drop.

that the velocity term in N_{Re} be taken as $|\bar{v}_o + \bar{v}_{f.c.}|$ where $\bar{v}_{f.c.}$ is a velocity component due to free convection parallel to gravity. If $|\bar{v}_{f.c.}|$ is taken equal to $(D_p g \beta \Delta t)^{1/2}$, Equations (8) and (9) for $v_o = 0$ become

$$N_{Nu}' = 2.0 + K_1(N_{Sc})^{1/3}(N_{Gr})^{1/4}$$

(10)

$$N_{Nu} = 2.0 + K_2(N_{Pr})^{1/3}(N_{Gr})^{1/4}$$

(11)

These are consistent with standard empirical correlations for free convection (22), at least insofar as the functional form of N_{Gr} is concerned.

Surface Conditions. In order to calculate evaporation rates, surface temperatures, t_i, and/or surface partial pressures, p_{Ai}, must be known. To estimate t_i and p_{Ai} a simultaneous graphical solution of two equations must be made. One of these equations is the temperature vapor-pressure relationship, and the other equation is a balance between the rate of heat and mass transfer. These equations may be written as follows:

$$p_{Ai} = p_{Ai}(t_i)$$

(12)

and

$$k\Delta t N_{Nu}(N_{Re}, N_{Pr})/D_p + \sigma\epsilon (T_r^4 - T_i^4)$$

$$= \lambda_i D_v \rho \Delta p_A N_{Nu}'(N_{Re}, N_{Sc})/M_m D_p p_f$$

(13)

where Equation (13) equates the heat

transferred by conduction, convection, and radiation to the latent heat of evaporation. Either side of the equation may be used to represent the evaporation rate.

For simultaneous heat and mass transfer under conditions of large temperature and concentration driving forces, corrections for sensible heat carried by the vapor molecules and diffusion due to thermal gradients must be taken into account (5). Such effects were negligible in this study.

Effect of Dissolved and Suspended Solids. When a droplet contains dissolved materials which lower the normal vapor pressure of the liquid, p_{Ai} is not only a function of t_i but also a function of the concentration of the nonvolatile component in the surface liquid. The net result is to lower Δt and Δp_A, such that the evaporation rate becomes lower than that for pure drops of the same size. This effect would not be expected for solutions or suspensions of inert materials, and drops containing such materials can be treated as evaporating at the same rate as pure drops of the same size.

When the normal vapor pressure of the liquid is lowered by dissolved solids, it can be assumed that the drop evaporates at any average concentration as though it were saturated throughout. Hence partial pressure for saturated solutions can be used in Equation (12). This simplification is based on the fact
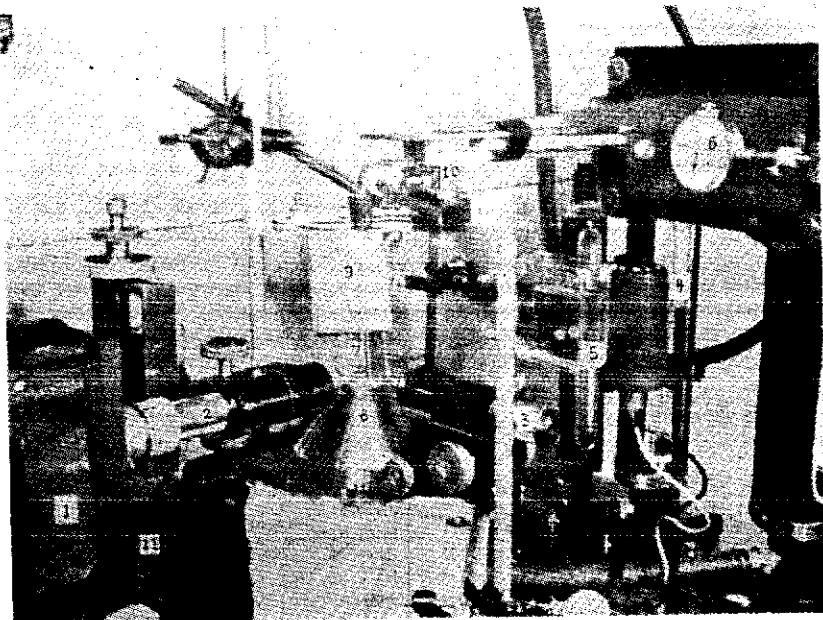
Fig. 2. Photograph of experimental equipment.

1. Micam camera.
2. Projection microscope
3. Viewing microscope.
4. Projection light.
5. Filter.
6. Microburet.
7. Suspension capillary.
8. Nozzle.
9. Thermoelement carrier.
10. Traversing mechanism.
11. Cold junction.

that diffusion coefficients in water are on the order of 10^{-5} sq.cm./sec., so small that solids will concentrate in the surface by evaporation much faster than they can diffuse toward the center of the drop.

If the heat evolved by crystallization is significant in comparison with the latent heat of evaporation, then the constant-rate period must be treated as two separate periods with a different surface temperature for each period. The first period can be treated as before. In the second period during crystallization, t_i
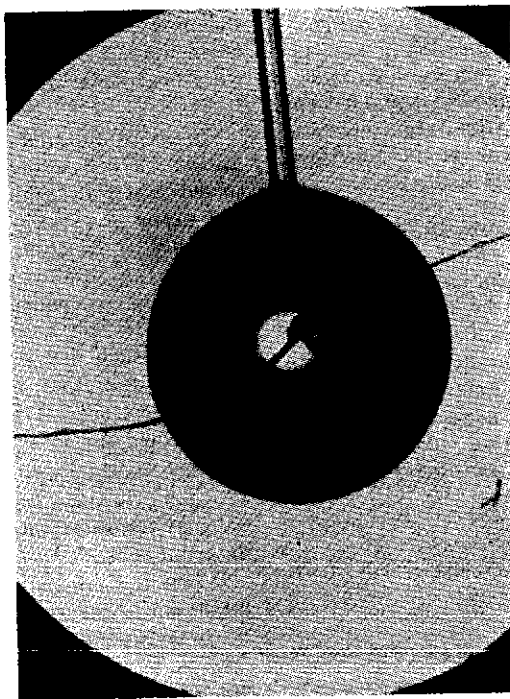

Fig. 3. Photomicrograph of an evaporating water drop, suspended from a feed capillary, with a ½ mil manganin-constantan thermoelement junction at its center. $D_p = 0.0945$ cm., capillary diam. about 80 μ.

must be calculated from an energy balance which includes the heat of crystallization. This heat contributes to evaporation and increases t_i. Although Δt is smaller, the rate of evaporation is lower since the total amount of heat being supplied for evaporation is larger and p_{At} has increased. From a treatment analogous to that of Williams and Schmitt (30), a heat balance gives

$$\lambda_i D_v \rho \Delta p_A N_{Nu}'(N_{Re},N_{Sc})/D_p M_m p_f$$

$$= k\Delta t N_{Nu}(N_{Re},N_{Pr})/D_p +$$

$$CD_v \rho \Delta p_A N_{Nu}'(N_{Re},N_{Sc})/D_p M_m p_f$$

$$(14)$$

where the effect of radiation is neglected and C is the heat evolved by crystallization per unit quantity of water evaporated from a saturated solution.

Since N_{Nu} is nearly equal in value to N_{Nu}' for water vapor in air, the ratio of vapor pressure difference to temperature difference for crystallizing aqueous solutions becomes

$$\frac{\Delta p_A}{\Delta t} = -\frac{kM_m p_f}{(\lambda_i - C)D_v \rho} \quad (15)$$

Thus, if C is significant, the slope of the wet-bulb line, given by Equation (15), is increased; and the temperature t_i, where it crosses the curve for the vapor pressure over a saturated salt solution, is also increased.

Experimental Equipment, Procedures, and Measurements

Rates of evaporation and heat transfer were obtained by a microtechnique in which drops of about one millimeter diameter were suspended from a microburet in a vertical, upward-flowing stream of air. Evaporation rates were determined by measuring the rate of feed through the buret necessary to maintain a constant-drop diameter. The temperature of the drop and the air stream were measured with small thermoelements. Evaporation rates in still air were determined in a special dryer. Suspended drops with decreasing diameters were evaporated in hot air streams and in still air, and the rate of evaporation was observed through a microscope and recorded on motion picture film.

The Air Stream and Measurement of Air Velocity. Metered dry air entered the bottom of a vertical 3¼-in. I.D., insulated tube, passed through a 200-w. electric heater, and then through a 4-in. depth of 4-mm. glass beads for distribution and an additional 4-in. depth of copper turnings for temperature stability. The tube was 40-in. long and terminated in a smoothly convergent nozzle of a shape suggested by Maché and Hebra (19). The nozzle opening was covered by a 140-mesh copper screen which made the velocity uniform over the opening and everywhere equal to the average volumetric velocity.

For velocities less than 300 cm./sec. point velocity mapping with a hot wire anemometer of the type used by King (16) showed that the screen evened the velocity distribution to the point where the volu-

metric rate through the flow meter gave an accurate measure of the central velocity. Velocity profiles taken 0.2 cm. above the nozzle persisted to some distance. The anemometer did not detect velocity fluctuations over the screen until the wire was less than 0.1 cm. from the opening. No indication of increased transfer due to turbulence created by the screen was noted in any of the tests.

Evaporation tests with air temperatures between 85° and 220° C. were made by suspending a drop on a fine filament over a hot, dry air stream and recording the history of evaporation on motion picture film. The hot air stream issued from a 25-mm. I.D. glass tube clamped to a swinging arm, and was moved under the suspended drop at the moment an evaporation test was started. The tube was filled with glass beads and covered with a 140-mesh screen, so that a uniform distribution of velocity could be assumed.

Method of Drop Suspension. Drops were suspended from a glass capillary, sealed to the delivery tube of a microburet, which had a capacity of 0.01 ml. in units of 10^{-5} ml. The capillaries were drawn so that the large end was the size of the ground glass tip of the microburet and the small end was 60 to 100μ in diameter. Since a drop would climb up the side of a plain glass capillary, they were coated with No. 9987 Dri-film to ensure that the drop hung freely from the tube.

This type of suspension system seemed to duplicate most nearly the case of a free drop. Much more than half the evaporation occurred on the side facing the air stream, and in this system the side presented to the air stream showed no protuberances. In addition, it was reasonable to believe that nearly the same type of eddying as that for a free drop occurred on the rear side, in contrast to what might be obtained if, for example, the drops were supported on horizontal wires or filaments. The suspended drop rotated at a linear velocity which appeared to be less than one per cent of the air velocity, and the rotation did not seem to be affected by the presence of the capillary. The effect of rotation was negligible in these experiments as it probably is in the evaporation of free drops falling at low Reynolds number.

Figure 2 shows the buret in place with the capillary positioned vertically over the center of the nozzle opening. The bottom of the drop cleared the screen about 0.3 cm. Evaporation rates for constant diameter drops were determined by measuring the rate of feed through the buret necessary to maintain a constant diameter.

Measurement of Drop Diameter. Figures 2 and 4 show pictures of the illumination and projection system used to observe the evaporating drop and measure its diameter. The drop image was projected and measured on the ground glass screen of a microscope camera. Figure 3 is a photograph of a drop as it appeared on the camera screen. Another microscope with long focal length objective and high-power eyepiece was used to observe the drop in reflected light and to aid in centering the thermoelement inside the drop. With room-temperature air, the diameter of a drop was easily kept within a tolerance of ±0.03 cm. on the screen.

In tests with hot air and changing drop diameter, motion pictures were taken at a magnification of approximately 7 times on the film, and at a rate of 24 frames/sec. Drop diameters were measured frame by frame on a microfilm viewer. In this case,
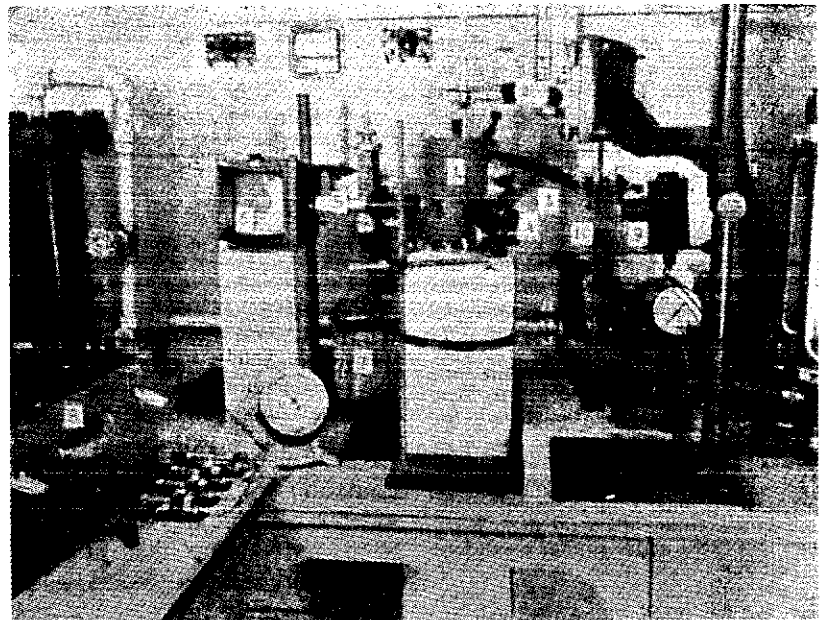

Fig. 4. Equipment for evaporation of drops in still air.

1. Special dryer.
2. Microburet.
3. Thermoelement carrier.
4. Observation microscope.
5. Projection microscope.
6. Micam camera screen.
7. Cold junction.
8. Potentiometer.
9. Projection light.
10. Filter.

diameter and time measurements were a measure of the evaporation rate.

Measurement of Air Temperature and Drop Temperature. Air temperatures and drop temperatures were measured with calibrated thermoelements of 3 mil, 2 mil, 1 mil, and ½ mil manganin-constantan wire. The thermocouples were held between needles mounted in a wood block which was carried by a traversing mechanism that made it possible to move the

junction in a horizontal plane above the nozzle (see Figure 2). Four couples were usually in operation at one time, 2 mil, 1 mil, and ½ mil wires being employed in series for extrapolation to a true temperature. It is believed that temperature readings to the nearest 0.1° C. were obtained.

During any one run (from 5 to 20 min.) the temperature of the air stream, measured by the fine thermoelements, never varied more than 0.2° C, and in most cases less than 0.1° C. The air temperature was
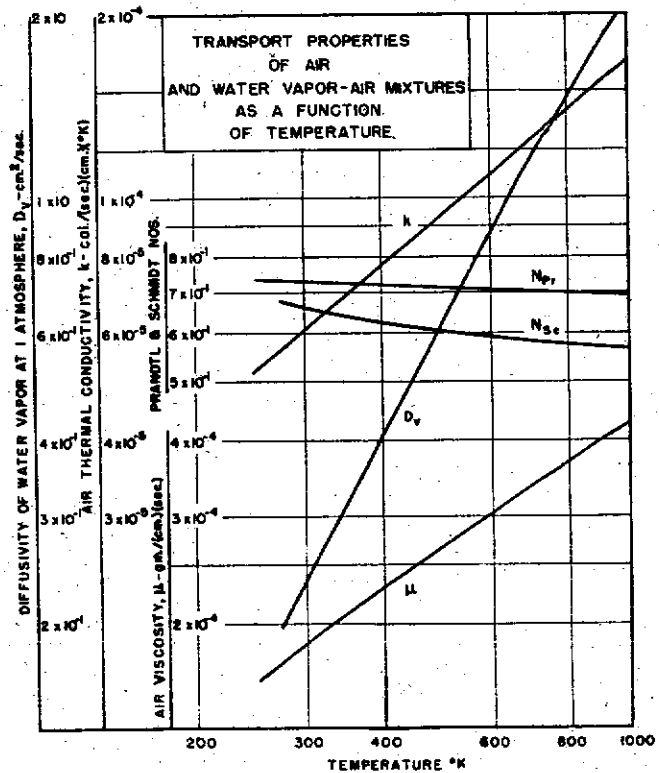

Fig. 5.

taken as the average temperature for the complete test run.

The temperature of the drop was measured by embedding a thermoelement junction inside the drop (see Figure 3). The junction had to be perfectly clean to accomplish this feat.

The thermocouple and its leads, the capillary, and the addition of sensible heat in the feed liquid, complicated the heat balance. An attempt was made to determine the magnitude of these various factors by taking temperature measurements under special conditions, for example, while feeding, while not feeding, with the capillary in place, and with the drop hanging from the thermoelement junctions. During evaporation tests, the thermoelement was removed so as not to disturb the flow pattern and provide an additional path for heat conduction. Consequently, the drop temperature for a test run was determined before the test by taking drop temperatures with 2-mil, 1-mil, and ½-mil thermoelements centered in a constant diameter drop being fed and evaporated under similar conditions as the test run.

For tests at 85° to 220° C., the air temperature was measured with a high velocity copper-constantan thermocouple at the center line, 0.3 cm. above the opening of the swinging air jet, and the drop temperature was approximated in separate tests by rapidly taking temperatures of drops suspended on thermoelements after the hot air stream was swung under the drop.

In every case measured drop temperatures were, for practical purposes, the same as wet bulb temperatures estimated from a standard psycrometric chart. The error in Δt's approximated from a psycrometric chart was never more than 4% for forced convection.

Measurement of Evaporation from Drops in Still Air

Figure 4 shows a special dryer for the study of evaporation rates in still air. The bottom and upper portions of the drying unit with the exception of observation windows and probe holes were filled with silica gel, and the entrance holes for the thermoelement apparatus and buret tip were sealed with plasticine.

The drop evaporated with changing diameter as it hung on a thermoelement or with constant diameter as it hung on a capillary. The temperature difference, Δt, was determined by an opposed-type thermoelement with junctions on a horizontal line one centimeter apart; the drop was suspended on one of the junctions.

Transport Properties of Air and Water Vapor

A critical review of the transport properties of air and water vapor was made to ensure reliable correlations of experimental data. The values used in calculations are given in graphical form by Figure 5, and the correlations presented later are dependent on these values.

Specific heats at constant pressure were taken from statistical mechanical calculations (6). Viscosity values were obtained by calculations based on the Lennard-Jones intermolecular potential (3, 12) and are in close agreement with careful experimental measurements (2, 13, 28). Values of thermal conductivity

are from the experimental data of Taylor and Johnson (26), the values for temperatures above 380° K. being obtained by extrapolation.

Recommended values of the diffusion coefficient of water vapor in air were calculated as a first approximation by R. B. Bird (12) from experimental measurements of the dipole moment and second virial coefficient of steam and the polarizability of air. The calculated values agree excellently with the original data of Winklemann (31) both in magnitude and temperature dependency but are approximately 10 per cent lower than that indicated by the S.T.P. value given by the International Critical Tables. A wide scattering of experimental values of diffusivity for air-water vapor mixtures are available, the latest work being that of Schirmer

$$q_{ai} = \lambda_i r_{Asi} = h_c \Delta t$$
$$+ r_{Asi} C_i \Delta t$$
$$+ \sigma \epsilon (T_s{}^4 - T_i{}^4)$$
$$+ r_{Asi} \lambda_i \left[\frac{\Delta(\Delta p_A)}{\Delta p_A} \right]_c$$

Equation (17) in terms of the Nusselt number becomes

$$N_{Nu} = \frac{h_c D_p}{k} = \frac{r_{Asi} \lambda_i D_p}{\Delta t\, k} \left\{ 1 - \frac{\Delta t C}{\lambda_i} - \frac{\pi \epsilon 4 T_s{}^3 \Delta t}{\lambda_i r_{Asi}} - \left[\frac{\Delta(\Delta p_A)}{\Delta p_A} \right]_s \right\} \qquad (18)$$

(25). However, every experimental method has involved a liquid-gas interface and a diffusion path of indefinite length. Because of such experimental difficulties (all the expected errors tend to give high values for D_v), because of the experimental value of N_{Nu}' at $N_{Re} = 0$ obtained in this study, and because of the greater consistency in calculated and experimental wet-bulb temperatures in this and related mass-transfer operations, the theoretical values of D_v listed here are considered to be the most accurate. The only other phenomenon which could explain the observed facts and cause a high apparent D_v would be the modification of the widely accepted assumption that the partial pressure of vapor at a liquid surface of temperature t_i is the equilibrium vapor pressure at temperature t_i. This implies an accommodation coefficient of 1.0, which may or may not be true for water surfaces (9).

Calculation Procedures

To determine the experimental value of N_{Nu} or $N_{Nu'}$ a major assumption made was that the surface temperature of the drop, t_i, was everywhere the measured value, and that the partial pressure of water vapor at the surface p_{Ai} was everywhere equal to the saturation partial pressure of water vapor at t_i. Since the thermal conductivity of water at 20° C. is 1.43×10^{-3} cal./(sec.) (cm.) (° C.) or 25 times as great as that of air, the temperature of the drop was assumed uniform throughout and equal to the experimentally measured temperature.

Actual measurements showed that the position of the thermoelement junction within the drop had no apparent effect on the indicated temperature.

The Nusselt group for mass transfer was determined by inserting the experimentally determined values and transport properties in the following equation:

$$N_{Nu'} = \frac{r_{Asi} D_p M_m p_t}{\Delta p_A D_{vp} \rho} \qquad (16)$$

Since water vapor at most represented but one per cent of the gas mixture, the physical properties of the transfer path were taken as those of dry air at the arithmetic average temperature. No correction was made for the cross-sectional area of the capillary since it represented less than 0.2 per cent of the drop surface.

The Nusselt number for heat transfer was more difficult to obtain since sensible heat added in the feed, transferred by conduction along the capillary, and brought in by radiation had to be considered. Since the heat transferred by all methods must equal the latent heat of evaporation, a heat balance gives

(convection and conduction)
(sensible heat)
(radiation)
(conduction along capillary)   (17)

where $(\Delta(\Delta p_A)/\Delta p_A)_c$ is the percentage change in Δp_A caused by the presence of the capillary. This fractional change in partial pressure difference was determined by drop temperature measurements with and without the capillary in place. Equation (18) shows the true value of N_{Nu} as an apparent N_{Nu} corrected by a series of terms. For a typical test (No. 80) the values of the correction terms were as follows:

$$N_{Nu} = 5.83(1 - 0.028 - 0.006 - 0.011)$$
$$= 5.57$$

Since the corrections for radiation and capillary effects were small, and since the correction for sensible heat was excessive (about half of it was actually realized), only the sensible heat correction was made for the points on the correlation curve, the errors in this procedure tending to cancel one another.

Although evaporation and heat-transfer rates in still air were obtained at constant diameter, it was considered more accurate to support the drop on a fine thermoelement and determine evaporation rates from the change in drop diameter with time. From such measurements the Nusselt groups can be determined from the relations

$$N_{Nu} = -\frac{1}{4} \frac{\lambda_i \rho_i}{\Delta t\, k} (dD_p{}^2/d\tau) \qquad (19)$$

$$N_{Nu'} = -\frac{1}{4} \frac{\rho_i M_m p_t}{\Delta p_A D_v \rho_M} (dD_p{}^2/d\tau) \qquad (20)$$

Equations (19) and (20) can be used also in the analysis of diameter vs. time data for drops evaporating at finite air velocities. In such an application the derivative of $D_p{}^2$ with respect to time varies with the instantaneous drop size.

Part II, to be run in an early issue, will contain Notation, Literature Cited, remaining figures and all tables.